

Location-Aware Predictive Beamforming for UAV Communications: A Deep Learning Approach

Chang Liu^{ID}, *Member, IEEE*, Weijie Yuan^{ID}, *Member, IEEE*, Zhiqiang Wei^{ID}, *Member, IEEE*,
Xuemeng Liu, and Derrick Wing Kwan Ng^{ID}, *Fellow, IEEE*

Abstract—The cellular-connected unmanned aerial vehicle (UAV) communication becomes a promising technique to realize the beyond fifth generation (5G) wireless networks, due to the high mobility and maneuverability of UAVs which can adapt to heterogeneous requirements of different applications. However, the movement of UAVs impose a unique challenge for accurate beam alignment between the UAV and the ground base station (BS). In this letter, we propose a deep learning-based location-aware predictive beamforming scheme to track the beam for UAV communications in a dynamic scenario. Specifically, a long short-term memory (LSTM)-based recurrent neural network (LRNet) is designed for UAV location prediction. Based on the predicted location, a predicted angle between the UAV and the BS can be determined for effective and fast beam alignment in the next time slot, which enables reliable communications between the UAV and the BS. Simulation results demonstrate that the proposed scheme can achieve a satisfactory UAV-to-BS communication rate, which is close to the upper bound of communication rate obtained by the perfect genie-aided alignment scheme.

Index Terms—Cellular-connected UAV communications, predictive beamforming, deep learning, location awareness.

I. INTRODUCTION

THE CELLULAR-CONNECTED unmanned aerial vehicle (UAV) communication, where a UAV is deployed as an aerial user equipment (UE) and served by ground base stations (BSs) has become one of the key enabling techniques for enhancing the network coverage, energy-efficiency, and capacity in the beyond fifth-generation (5G) wireless networks [1], [2]. Relying on its high maneuverability, a UAV can help BSs in different areas to fulfill various applications, such as photography, mapping, and surveying [3]. In most practical scenarios, multi-antenna systems are adopted to

facilitate UAV communications. Therefore, the beamforming technique, through which an antenna array can establish directional energy-focusing beams at specific angles to improve the communication efficiency, is of great importance for high data-rate transmission in cellular-connected UAV communications and thus it has attracted extensive attention from both academia and industry [4].

In the literature, effective algorithms and schemes have been proposed for addressing the beamforming problem in cellular-connected UAV communications. For instance, in [5], a hybrid beam tracking approach was proposed for the beam alignment in UAV-to-satellite links. In the proposed scheme, several sensors are mounted on the UAV to obtain navigation information for beam alignment, which however, are not always practical due to the size and power limitation on UAVs. In addition, [6] proposed a position-based lightweight beamforming scheme for 5G UAV broadcasting communications, where a global positioning system (GPS)-assisted beam tracking approach was studied for the beam alignment in BS-to-UAVs links. Nevertheless, the deployment of the GPS is costly and complicated, which is not always realizable for UAVs. As an alternative, pilot-based methods have been developed to facilitate beam alignment. For example, the authors in [7] jointly adopted both the beam training and the velocity estimation to optimize a pilot-based beam tracking scheme for beam alignment. Also in [8], a three-dimensional beamforming algorithm was designed by applying the dynamic pilot insertion. However, for high-speed UAVs, due to the relatively long delay required in pilot transmission, these pilot-based methods cannot capture the up-to-date UAV locations in a timely manner and only achieve a limited beam tracking performance. More importantly, the high maneuverability of UAVs introduces a wide possible range of trajectory, which complicates the task of beam alignment. Hence, a more practical beam alignment scheme, which can response timely and is suitable for various UAV trajectories, is desired.

Note that the UAV location changes with time and its current location highly depends on its previous locations, i.e., the UAV locations are temporally correlated. Thus, the UAV trajectory can be regarded as a temporally correlated sequence. On the other hand, the deep learning (DL) technique [9], especially the long short-term memory (LSTM) neural network, has powerful capability of exploiting the temporal dependencies. Motivated by this, in this letter, we propose a DL-based location-aware predictive beamforming scheme to facilitate the beam alignment in cellular-connected UAV communications. In the proposed scheme, an LSTM-based recurrent neural network (LRNet) is specifically designed to exploit the temporal dependency of the UAV trajectory sequences for UAV location prediction. In contrast to existing beam alignment

Manuscript received November 11, 2020; revised December 11, 2020; accepted December 13, 2020. Date of publication December 16, 2020; date of current version March 9, 2021. The work of Chang Liu was supported by the National Natural Science Foundation of China under Grant 61801082. The work of Derrick Wing Kwan Ng was supported in part by the UNSW Digital Grid Futures Institute, UNSW, Sydney, under a cross-disciplinary fund scheme and in part by the Australian Research Council's Discovery Project under Grant DP190101363. The associate editor coordinating the review of this article and approving it for publication was J. Tang. (*Corresponding author: Weijie Yuan.*)

Chang Liu, Zhiqiang Wei, and Derrick Wing Kwan Ng are with the School of Electrical Engineering and Telecommunications, University of New South Wales, Sydney, NSW 2052, Australia (e-mail: chang.liu19@unsw.edu.au; zhiqiang.wei@unsw.edu.au; w.k.ng@unsw.edu.au).

Weijie Yuan was with the School of Electrical Engineering and Telecommunications, University of New South Wales, Sydney, NSW 2052, Australia. He is now with the Department of Electrical and Electronic Engineering, Southern University of Science and Technology, Shenzhen 518055, China (e-mail: weijie.yuan@unsw.edu.au).

Xuemeng Liu is with the School of Electrical and Information Engineering, University of Sydney, Sydney, NSW 2006, Australia (e-mail: xliu2557@uni.sydney.edu.au).

Digital Object Identifier 10.1109/LWC.2020.3045150

methods, e.g., [5]–[8], the proposed scheme neither requires the use of pilots nor navigation sensors. Instead, only an LRNet-based offline training is required to exploit the temporal features of the UAV trajectory for accurate location prediction [10]. Based on the predicted location, a predicted angle between the UAV and the BS can be determined for the beam alignment in the next time slot, which enables reliable UAV communications. Simulation results demonstrate that the proposed predictive beamforming scheme can accurately predict the UAV location for beam alignment and achieve a stable communication rate for the UAV-to-BS link.

Notations: Terms \mathbb{R} and \mathbb{C} are the sets of the real numbers and the complex numbers, respectively. The superscripts T and H are used to represent the transpose and the conjugate transpose, respectively. $|\cdot|$ and $\|\cdot\|$ denote the modulus of a complex number and the Euclidean norm of a vector. \mathbf{I} and $\mathbf{0}$ denote the identity matrix and the zero vector, respectively. $U(a, b)$ denotes the uniform distribution with the range between a and b ($a \leq b$). $\mathcal{N}(\boldsymbol{\mu}, \boldsymbol{\Sigma})$ denotes the Gaussian distribution with mean vector $\boldsymbol{\mu}$ and covariance matrix $\boldsymbol{\Sigma}$. $\arccos(\cdot)$ is the inverse cosine function.

II. SYSTEM MODEL

The considered UAV-to-BS communication scenario is illustrated in Fig. 1. The UAV is equipped with an M -antenna uniform linear array (ULA) hovering in the sky and communicating with a static BS with an N -antenna ULA.¹ For ease of exposition, we assume that the ULAs of the UAV and the BS are in parallel, then the angle-of-arrival (AOA) is identical to the angle-of-departure (AoD) [5]. Without loss of generality, the coordinate of the BS is set as $\mathbf{x}_p = [x_p, y_p]^T$, where x_p and y_p are the coordinates on x -axis and y -axis, respectively. The location of the moving UAV at time instant k is denoted by $\mathbf{u}_k = [x_k, y_k]^T$. Consequently, the angle of the UAV relative to the BS at time k is given by

$$\theta_k = \arccos \frac{x_k - x_p}{\|\mathbf{u}_k - \mathbf{x}_p\|}, \quad (1)$$

as shown in Fig. 1.

For practical UAV communications, a rich scattering scenario rarely appears [3], therefore, the UAV-to-BS channel consists of only the line-of-sight (LOS) communication link, denoted by a channel matrix $\mathbf{H}_k \in \mathbb{C}^{N \times M}$, i.e.,

$$\mathbf{H}_k = \frac{c}{4\pi f_c \|\mathbf{u}_k - \mathbf{x}_p\|} \mathbf{b}(\theta_k) \mathbf{a}(\theta_k)^H, \quad (2)$$

where \sqrt{MN} is the antenna array gain, c is the signal propagation speed, f_c is the centre carrier frequency, and $\mathbf{a}(\theta_k)$ and $\mathbf{b}(\theta_k)$ denote the normalized transmitting and receiving steering vectors, respectively. In particular, the antenna spacing for ULAs of both the UAV and the BS can be set as $d_c = \frac{f_c}{2c}$. Therefore, we have

$$\mathbf{a}(\theta_k) = \left[1, e^{-j \frac{2\pi d_c \cos \theta_k}{\lambda_c}}, \dots, e^{-j \frac{2\pi d_c (M-1) \cos \theta_k}{\lambda_c}} \right]^T, \quad (3)$$

¹Multiple UAVs can be considered if each UAV is equipped with a massive antenna system, in this case, the steering vectors from different UAVs are asymptotically orthogonal. For ease of investigation, we consider a single UAV scenario, which can be extended to multi-UAV scenario straightforwardly at the expense of more involved notations.

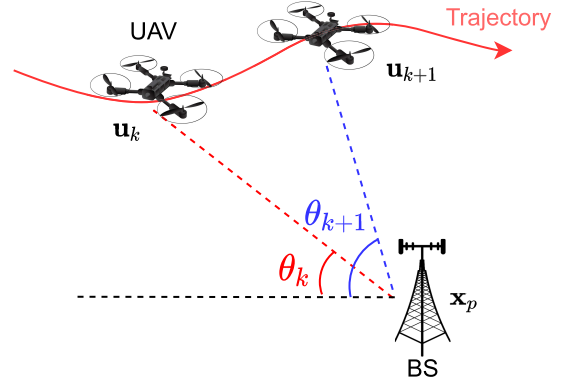


Fig. 1. UAV communication model.

$$\mathbf{b}(\theta_k) = \left[1, e^{-j \frac{2\pi d_c \cos \theta_k}{\lambda_c}}, \dots, e^{-j \frac{2\pi d_c (N-1) \cos \theta_k}{\lambda_c}} \right]^T, \quad (4)$$

where we set $\lambda_c = 2d_c$ for simplifying the steering vectors.

Assume that k denotes the current time slot, let us denote the transmitted signal from the UAV at time k by $s_k \in \mathbb{C}$. The transmitted signal is steered towards the intended direction via a transmit beamformer \mathbf{f}_k and propagates through the channel \mathbf{H}_k . After receiving the signal, the BS adopts a receive beamformer \mathbf{w}_k and obtains the received sample r_k as

$$r_k = \mathbf{w}_k^H \mathbf{H}_k \mathbf{f}_k s_k + \eta_k, \quad (5)$$

where $\eta_k \in \mathbb{C}$ is the noise variable with zero mean and variance σ^2 . In general, the transmit beamformer adopted at the UAV can be designed based on the relative angle θ_k , i.e., $\mathbf{f}_k = \sqrt{\frac{1}{M}} \mathbf{a}(\theta_k)$, since the UAV can obtain its location information at each time slot. In contrast, the BS can only obtain an estimated angle $\hat{\theta}_k$ based on the previous UAV locations, i.e., $\{\mathbf{u}_{k-L}, \dots, \mathbf{u}_{k-1}\}$, which are sent by the UAV at the previous time slots. Based on $\hat{\theta}_k$, the receive beamformer at the BS can be expressed as $\mathbf{w}_k = \sqrt{\frac{1}{N}} \mathbf{b}(\hat{\theta}_k)$. According to (5), the receive signal-to-noise ratio (SNR) is given by

$$\begin{aligned} \text{SNR}_k &= \frac{p_t |h_k \mathbf{w}_k^H \mathbf{b}(\theta) \mathbf{a}(\theta)^H \mathbf{f}_k|^2}{\sigma^2} \\ &= \frac{M p_t |h_k \mathbf{w}_k^H \mathbf{b}(\theta)|^2}{\sigma^2}, \end{aligned} \quad (6)$$

where $p_t = |s_k|^2$ denotes the transmit signal power and $h_k = \frac{c}{4\pi f_c \|\mathbf{u}_k - \mathbf{x}_p\|}$ is the path loss gain at time k . The achievable rate of the UAV-to-BS link at time k is therefore given by

$$R_k = \log_2(1 + \text{SNR}_k). \quad (7)$$

We can observe from (6) that if the predicted angle $\hat{\theta}_k$ equals to the actual angle θ_k , the SNR as well as the achievable rate is maximized. However, due to the dynamic nature of the UAV, the angle θ_k is time-varying which imposes a challenge on obtaining accurate beam alignment. In the next section, we will propose a learning-based predictive beamforming algorithm to predict the UAV location at the BS side and consequently obtain the predicted angle $\hat{\theta}_k$. Thus, the UAV and the BS can directly establish the communication link through beam alignment at time k .

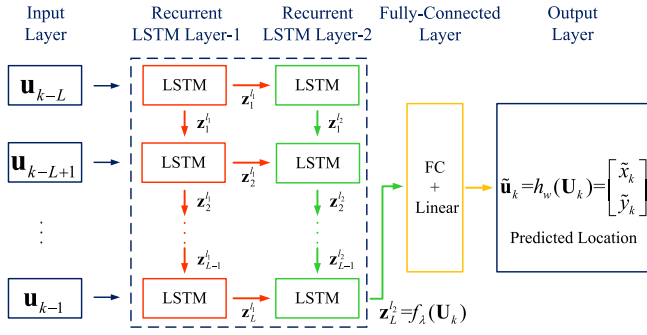


Fig. 2. The proposed LRNet for location prediction.

III. LOCATION-AWARE PREDICTIVE BEAMFORMING

The proposed predictive beamforming scheme consists of the location prediction step and the beamforming design step. First, the UAV location is predicted at the BS via a neural network in the prediction step. Then, this information is adopted for beam alignment in the beamforming design step.

Generally, the movement of the UAV can be modeled as [4]

$$\mathbf{u}_k = \mathbf{u}_{k-1} + \mathbf{v}_{k-1} \Delta T + \mathbf{\Lambda}_{k-1}. \quad (8)$$

Here, $\mathbf{v}_{k-1} = [v_{k-1}^x, v_{k-1}^y]^T, \forall k$, denotes the UAV average velocity at time $k-1$, where v_{k-1}^x and v_{k-1}^y are the projections on the x -axis and y -axis, respectively. Let $\alpha_{k-1} = \|\mathbf{v}_{k-1}\|$ and $\beta_{k-1} = \arccos(\frac{v_{k-1}^x}{\|\mathbf{v}_{k-1}\|})$ denote the amplitude and phase of \mathbf{v}_{k-1} , respectively. Without loss of generality, the amplitude and the phase are assumed to follow the uniform distribution [4], i.e., $\alpha_{k-1} \sim U(a, b)$ and $\beta_{k-1} \sim U(c, d)$, where a, b, c, d are constants with $0 \leq a \leq b$ and $-\pi \leq c \leq d \leq \pi$. Also, ΔT represents the time duration of a time slot. In addition, considering that random wind gust may cause the UAV location deviation, we then introduce $\mathbf{\Lambda}_{k-1} = [\rho_{k-1}^x, \rho_{k-1}^y]^T$ to characterize the environment uncertainty at time $k-1$, where ρ_{k-1}^x and ρ_{k-1}^y are the uncertainty offsets on the x -axis and y -axis, respectively. In addition, $\mathbf{\Lambda}_{k-1} \sim \mathcal{N}(\mathbf{0}, \sigma_v^2 \mathbf{I})$ is assumed to be a Gaussian random vector and σ_v^2 is the variance depending on the wind [3].

Now, we propose a DL approach for predicting the UAV location at time k , which relies on the previous L locations, i.e., the location sequence $\{\mathbf{u}_{k-L}, \dots, \mathbf{u}_{k-1}\}$ sent by the UAV.

A. Deep Learning-Based Location Prediction

To fully exploit the temporal features of the UAV location sequence, an LRNet is proposed for location prediction. As shown in Fig. 2, the LRNet consists of an input layer, recurrent LSTM layer-1, recurrent LSTM layer-2, a fully-connected (FC) layer, and an output layer. The hyperparameters of the proposed LRNet are summarized in Table I and each layer will be introduced in the following.

1) *Input Layer*: Denote by

$$\mathbf{U}_k = [\mathbf{u}_{k-L}, \dots, \mathbf{u}_{k-1}] \quad (9)$$

the L -length location sequence. $\mathbf{U}_k \in \mathbb{R}^{2 \times L}$ carries the temporal location information and thus is used as the input of the LRNet.

2) *Recurrent LSTM Layers*: To exploit the long-term dependencies of the location sequence, two recurrent LSTM layers

TABLE I
HYPERPARAMETERS OF THE PROPOSED LRNET

Input: \mathbf{U}_k with the size of $2 \times L$		
Layers	Parameters	Values
LSTM layer-1	Size of $\mathbf{z}_i^{l_1}$	50×1
LSTM layer-2	Size of $\mathbf{z}_i^{l_2}$	100×1
FC layer	Activation function	Linear
Output: $\tilde{\mathbf{u}}_k$ with the size of 2×1		

are adopted, named recurrent LSTM layer-1 and recurrent LSTM layer-2, as shown in Fig. 2. For each recurrent layer, there are L identical LSTM modules cascaded handling the input from the input layer in the past L time steps, respectively. Besides, let \mathbf{z}_i^j represent the output of the LSTM of the j -th, $j \in \{1, 2\}$, layer at the i -th $i \in \{1, 2, \dots, L\}$ time step, we can then characterize the LSTM modules of different layers. For LSTM layer-1, the output $\mathbf{z}_i^{l_1}$ is not only sent to the next recurrent layer, but also saved as the input of the LSTM module at the next time step. For LSTM layer-2, the output $\mathbf{z}_i^{l_2}$ is only served as the input of the same LSTM module at the next time step. In particular, the L -th output $\mathbf{z}_L^{l_2}$ is the output of the LSTM layers which is expressed as

$$\mathbf{z}_L^{l_2} = f_\lambda(\mathbf{U}_k), \quad (10)$$

where $f_\lambda(\cdot)$ with parameters λ denotes a non-linear function characterizing the operation from LSTM layer-1 to LSTM layer-2.

3) *Fully-Connected Layer*: After the feature extraction from the two recurrent LSTM layers, a FC layer is then added between the recurrent LSTM layer-2 and the output layer to linearly combine these extracted features to further improve the network performance [11].

4) *Output Layer*: Based on the above analysis, the output of the LRNet can be expressed as

$$\tilde{\mathbf{u}}_k = \sigma(\mathbf{W}f_\lambda(\mathbf{U}_k) + \mathbf{b}), \quad (11)$$

where $\tilde{\mathbf{u}}_k \in \mathbb{R}^{2 \times 1}$ is the predicted location at time k by LRNet, $\mathbf{W} \in \mathbb{R}^{2 \times 100}$ and $\mathbf{b} \in \mathbb{R}^{2 \times 1}$ are the weights and bias of the FC layer, and $\sigma(\cdot)$ represents the linear activation function. For simplicity, we can rewrite (11) as

$$\tilde{\mathbf{u}}_k = h_w(\mathbf{U}_k) = \begin{bmatrix} \tilde{x}_k \\ \tilde{y}_k \end{bmatrix}, \quad (12)$$

where $h_w(\cdot)$ is the total expression of LRNet with parameters $w = \{\lambda, \mathbf{W}, \mathbf{b}\}$ and \tilde{x}_k and \tilde{y}_k are the elements of the predicted location as defined in (1).

In fact, the location prediction of (8) is essentially a regression problem. Inspired by this, a mean square error (MSE) cost function is selected for the proposed LRNet, which is expressed as [9]

$$J_{\text{MSE}}(w) = \frac{1}{2N} \sum_{n=1}^N \left\| \mathbf{u}_k^{(n)} - h_w(\mathbf{U}_k^{(n)}) \right\|^2, \quad (13)$$

where $\mathbf{u}_k^{(n)}$ and $\mathbf{U}_k^{(n)}$ represent the label and the input of the n -th, $n \in \{1, 2, \dots, N\}$, training example.² Therefore, we can then adopt a backpropagation algorithm [9] to update the parameters progressively to minimize J_{MSE} in (13) and finally obtain the well-trained LRNet for location prediction.

Note that the proposed LRNet is a versatile network structure which is robust for different scenarios. For example, if we choose different parameters (i.e., σ_v^2 , a , b , c , and d in (8)) for the UAV movement model, we can obtain a variety of training examples from different statistical distributions. In this case, the well-trained LRNet is suitable for different UAV movement scenarios, which further improves the robustness of the proposed LRNet. In addition, although the input size of the LRNet generally changes with L , the proposed LRNet structure can be easily extended to different shapes accordingly due to the high scalability of the neural network [9].

B. Predictive Beamforming Design

Based on the predicted location $\tilde{\mathbf{u}}_k$ from the LRNet, the BS is able to determine the predicted angle $\tilde{\theta}_k$ as

$$\tilde{\theta}_k = \arccos \frac{\tilde{x}_k - x_p}{\|\tilde{\mathbf{u}}_k - \mathbf{x}_p\|}, \quad (14)$$

and formulate the receive beam as $\mathbf{w}_k = \mathbf{b}(\tilde{\theta}_k)$. Based on this prediction mechanism, the UAV and the BS can directly establish the communication link at time k .

Moreover, the powerful DL-based prediction enables the BS to combat unexpected link failures. For example, given the previous states of the UAV, denoted by $\{\mathbf{u}_{k-L}, \dots, \mathbf{u}_{k-1}\}$, the BS can not only predict the UAV location at time k , but also a further step to $\tilde{\mathbf{u}}_{k+1}$. In a special circumstance that the UAV fails to report its location to the BS at time k , the BS can still exploit the predicted location $\tilde{\mathbf{u}}_{k+1}$ to formulate the receive beamforming at time $k+1$ for maintaining a reliable UAV-to-BS communication.

Remark 1: Note that this work focuses on a simple but important model which serves as a foundation for possible extension to different settings. For extending the current framework to a more complex scenario, we can consider a multi-UAV scenario. In addition, wind gusts in the air would introduce turbulence to the UAV, which leads to UAV jittering [12]. In fact, both the motions of the UAVs and the random UAV jittering effect can be taken into account in the proposed beam tracking algorithm design. However, due to the page limitation, we would like to keep the current problem formulation as it is since it serves as a solid foundation for the investigation of deep learning in UAV beam tracking and possible further extensions.

IV. SIMULATION RESULTS

This section presents the simulation results to verify the effectiveness of the proposed beamforming scheme. For

²Note that the adopted UAV movement model in (8) can well characterize the actual UAV trajectory [4]. Thus, label data for offline training can be generated by simulation based on (8). Moreover, although the unsupervised learning approach does not require the use of labels, a large training overhead is generally needed while achieving only a limited prediction accuracy compared with the supervised learning approaches [9]. Thus, to guarantee a high location prediction accuracy, we adopt the supervised learning approach in this letter.

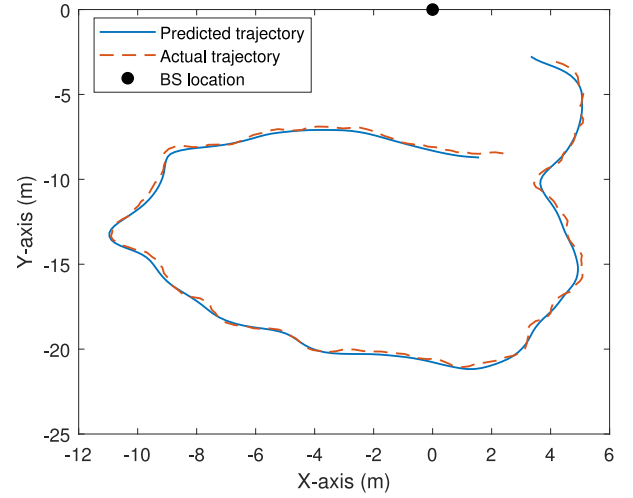


Fig. 3. Illustration of the actual and the predicted trajectories.

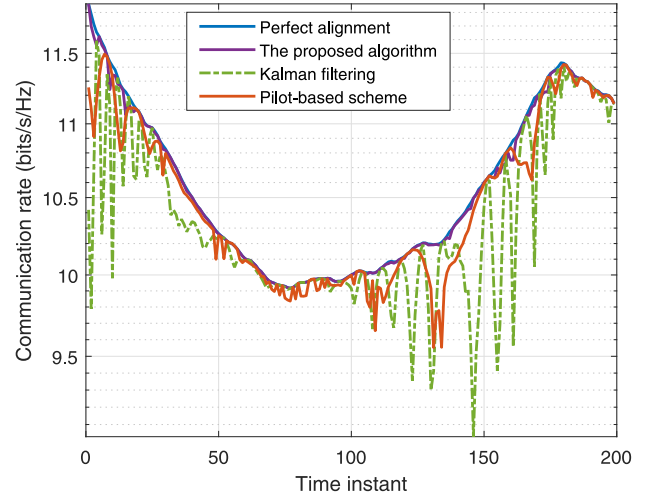


Fig. 4. The comparison of the communication rate between the baseline schemes and the proposed approach.

brevity, we assume that the location of the BS is fixed at $\mathbf{x}_p = [0, 0]^T$. The ULA mounted on the UAV has $M = 16$ antennas while the BS is equipped with $N = 8$ antennas. The operating frequency for the considered UAV-BS system is $f_c = 30$ GHz. The transmit power p_t is set as 20 dBm and the thermal noise power is $\sigma^2 = -90$ dBm. We consider a total number of 200 time instants and the duration for each time instant is $\Delta T = 0.02$ s. The UAV movement model is given in (8) with $\sigma_v = 0.01$, and we set $a = 0.4$ m/ ΔT , $b = 0.7$ m/ ΔT , $c = -\pi/6$, and $d = \pi/6$, i.e., the UAV has an equivalent speed around 20~35 m/s [13]. Finally, we assume that the input length $L = 20$.

In Fig. 3, we show the actual trajectory of the UAV and the trajectory determined by the predicted locations of the UAV. We can see that relying on the LRNet, the BS is capable of efficiently predicting the location of the UAV in real-time. Even though the moving direction of the UAV varies rapidly at some time instants, we can observe that the location prediction error is around the level of 0.1 m at all time instants.

Fig. 4 depicts the communication rate of the proposed predictive beamforming approach. For comparison, we also plot the communication rates for three reference schemes.

TABLE II
COMPUTATIONAL COMPLEXITY OF DIFFERENT ALGORITHMS

Algorithm	Computational Complexity
Pilot-based scheme	$O(\Theta)$
Kalman filtering	$O(1)$
LRNet	$O\left(4L\left(\sum_{i=1}^2 m_i n_i + n_i^2 + n_i\right)\right)$

Specifically, the genie-aided perfect alignment scheme assumes that the estimated angle $\hat{\theta}_k$ is identical to the actual angle θ_k at each time instant. Obviously, this serves as the upper bound of the communication rate. Another baseline scheme predicts the UAV location via Kalman filtering based on the locations of the previous two time instants for determining the beamformer. We can observe from Fig. 4 that the proposed predictive beamforming scheme can establish a reliable communication link between the UAV and the BS. In particular, it can be seen that the rate of the proposed scheme decreases slightly at some instants due to a drastic change of the UAV location, which can be in general addressed by adopting a higher value of L in the LRNet [9]. In contrast, although the Kalman filtering-based scheme has a very simple process for predicting the UAV location, it suffers from severe rate degradation and huge rate fluctuation due to the mismatch of the receive beamformer and the channel. In practice, the fluctuations of the communication rate for the Kalman filtering-based prediction method would impose challenges for reliably transmitting information from the UAV to the BS. In particular, for some scenarios with strict rate requirement, e.g., video streaming, an outage event may occur due to the sharp rate degradation. On the other hand, as for the pilot-based beam alignment scheme, we consider the exhaustive search of the beam direction using one pilot symbol [7], [8]. It can be seen that the pilot-based scheme suffers from a significant performance loss compared to the proposed algorithm due to the limited searching precision in the pilot-based scheme.

In addition, we briefly compare the complexity for three different beam tracking algorithms, as summarized in Table II. To elaborate, the complexity for the classic pilot-based scheme depends on the exhaustive beam direction search process, which is roughly given by $O(\Theta)$, where Θ denotes the number of possible beam directions in the angular domain. Also, the complexity for the Kalman filtering-based prediction is relatively low since it is equivalent to the linear interpolation, having an order of complexity of $O(1)$. For the learning-based algorithm, m_i and n_i , $i \in \{1, 2\}$ represent the input and output sizes of each LSTM module in the LSTM layer- i of the proposed LRNet, respectively [12]. In addition, L denotes the number of time steps of LRNet. Note that although the proposed LRNet for location prediction involves a large number of parameters, its computational complexity is still in polynomial time. Indeed, the actual online prediction time can be greatly reduced through the parallelization of graphics processing unit (GPU). For example, when we send an arbitrary input to a well-trained LRNet for location prediction, its computation time on a desktop computer with an i7-6700

3.4 GHz central processing unit (CPU) and a Nvidia GeForce GTX 1080 GPU is $\tau_c = 2$ ms which is less than the observation time duration $\Delta T = 20$ ms. In fact, the computation time can be further reduced if tailor-made machine learning computation chips are adopted. Therefore, the BS can complete the prediction task before the next time instant, i.e., the complexity of the proposed LRNet is acceptable and the predicted trajectory can track the actual trajectory. Through this comparison, we can verify the effectiveness of the proposed approach in guaranteeing stable communications.

V. CONCLUSION

This letter studied the practical beam alignment problem for cellular-connected UAV communications and adopted a DL approach to develop a location-aware predictive beamforming scheme to track the beam for UAV communications in a dynamic scenario. The proposed predictive beamforming scheme design consists of the DL-based location prediction and the predictive beamforming. Specifically, an LRNet was designed to exploit the temporal features of the UAV trajectory for location prediction. Based on the predicted location, a beam alignment was designed for the next time slot to enable reliable communications between the UAV and the BS. Simulation results showed that the achievable communication rate of the proposed method approaches that of the upper bound of the communication rate obtained by the perfect alignment scheme.

REFERENCES

- [1] V. W. Wong, R. Schober, D. W. K. Ng, and L.-C. Wang, *Key Technologies for 5G Wireless Systems*. Cambridge, U.K.: Cambridge Univ. Press, 2017.
- [2] Q. Wu *et al.*, "5G-and-beyond networks with UAVs: From communications to sensing and intelligence," 2020. [Online]. Available: arXiv:2010.09317.
- [3] D. Xu, Y. Sun, D. W. K. Ng, and R. Schober, "Multiuser MISO UAV communications in uncertain environments with no-fly zones: Robust trajectory and resource allocation design," *IEEE Trans. Commun.*, vol. 68, no. 5, pp. 3153–3172, May 2020.
- [4] Y. Zeng, Q. Wu, and R. Zhang, "Accessing from the sky: A tutorial on UAV communications for 5G and beyond," *Proc. IEEE*, vol. 107, no. 12, pp. 2327–2375, Dec. 2019.
- [5] J. Zhao, F. Gao, Q. Wu, S. Jin, Y. Wu, and W. Jia, "Beam tracking for UAV mounted SatCom on-the-move with massive antenna array," *IEEE J. Sel. Areas Commun.*, vol. 36, no. 2, pp. 363–375, Feb. 2018.
- [6] W. Miao, C. Luo, G. Min, and Z. Zhao, "Lightweight 3-D beamforming design in 5G UAV broadcasting communications," *IEEE Trans. Broadcast.*, vol. 66, no. 2, pp. 515–524, Jun. 2020.
- [7] L. Yang and W. Zhang, "Beam tracking and optimization for UAV communications," *IEEE Trans. Wireless Commun.*, vol. 18, no. 11, pp. 5367–5379, Nov. 2019.
- [8] Y. Huang, Q. Wu, T. Wang, G. Zhou, and R. Zhang, "3D beam tracking for cellular-connected UAV," *IEEE Wireless Commun. Lett.*, vol. 9, no. 5, pp. 736–740, May 2020.
- [9] I. Goodfellow, Y. Bengio, A. Courville, and Y. Bengio, *Deep Learning*. Cambridge, MA, USA: MIT Press, 2016.
- [10] S. Hochreiter and J. Schmidhuber, "Long short-term memory," *Neural Comput.*, vol. 9, no. 8, pp. 1735–1780, Nov. 1997.
- [11] C. Liu, J. Wang, X. Liu, and Y.-C. Liang, "Deep CM-CNN for spectrum sensing in cognitive radio," *IEEE J. Sel. Areas Commun.*, vol. 37, no. 10, pp. 2306–2321, Oct. 2019.
- [12] W. Yuan, C. Liu, F. Liu, S. Li, and D. W. K. Ng, "Learning-based predictive beamforming for UAV communications with jittering," *IEEE Wireless Commun. Lett.*, vol. 9, no. 11, pp. 1970–1974, Nov. 2020.
- [13] Y. Kang and J. K. Hedrick, "Linear tracking for a fixed-wing UAV using nonlinear model predictive control," *IEEE Trans. Control Syst. Technol.*, vol. 17, no. 5, pp. 1202–1210, Sep. 2009.